PHYSICAL REVIEW B VOLUME 26, NUMBER 12 15 DECEMBER 1982

Theory of amorphous SiO_2 and SiO_x. I. Atomic structural models

W. Y. Ching
Department of Physics, University of Missouri-Kansas City, Kansas City, Missouri 64110
(Received 1 June 1982)

Based on existing periodic models for amorphous Si, a series of random-network models with periodic boundaries have been constructed for amorphous SiO_2 and SiO_x, with $x=1.5$, 1.0, and 0.5. The network structures in which an O atom always bonds to two Si atoms in a bridging position and a Si atom is tetrahedrally linked to four O atoms (for a-SiO_2) or both O and Si atoms (for SiO_x), are computer relaxed using a Keating-type of elastic potential. The resulting models have no internal voids or dangling bonds and have densities similar to the experimental values. Results are presented for the total and partial radial distribution functions, as well as for bond-angle and bond-length distributions and statistics of bonding patterns. For SiO_x with $x=1.0$, models are constructed according to both the random-bond concept and the random-mixture concept. Detailed examination of these two types of models indicates the former should be slightly more favored although the radial distribution functions of the two are quite similar. This conclusion is opposite to that reached by Temkin. Utilization of these periodic models for the study of electronic structures in a-SiO_2 and SiO_x is also discussed.

I. INTRODUCTION

The most fundamental information needed to understand the various properties of materials is the structural arrangement of the constituent atoms. In crystalline solids, the position of each atom in the unit cell can be accurately determined by x-ray diffraction in conjunction with the knowledge of a finite number of space groups associated with the long-range periodicity of the lattice. In a disordered solid, there is no long-range order and the structure is usually characterized by short-range order such as nearest-neighbor (NN) coordination numbers, average bond length, and bond angle of coordinated atoms and ring structures. In general, there is no unique set of atomic coordinates to describe the structure of amorphous materials. The ground-state configurations for a disordered material may be highly degenerate and separated from one another only by small energy barriers. We are actually facing a statistical ensemble of equally acceptable structural configurations. The experimentally measured radial distribution function (RDF) of amorphous materials can only provide partial information regarding their structures. In this situation, model construction based on various plausible atomic arrangements and subsequent study of material properties based on these models can provide insight into the nature and properties of disordered materials.

It has been generally accepted that for covalently bonded disordered materials such as amorphous silicon (a-Si) or amorphous silicon dioxide (a-SiO_2), the continuous random-network (CRN) model is the simplest reasonably appropriate model to describe their structures.[1] Very recently, a different school of thought based on topological argument has emerged[2] and occasionally, a microcrystallite model has also been advocated.[3] Model construction for a-SiO_2 based on the CRN theory began as early as the mid-sixties.[4] It was extended later to tetrahedrally bonded amorphous semiconductors[5,6] and to a lesser extent, chalcogenide materials.[7] Most of these models involve clusters of several hundred atoms with free surfaces, although quasi-periodic models (QPM) of modest sizes have also been constructed for a-Si.[8–10] It has been customary to compare the RDF calculated from the model structure with that measured experimentally to assess the suitability of the model. In general, agreement in the RDF is a necessary but not sufficient condition for a good model; a more discriminating test is to study the other physical observables based on the models constructed. In this respect, the QPM is particularly valuable because it represents a truly infinite array of network atoms free of surface effects. Furthermore, properties of each model such as density, ring structure, or

bond-length distortion can be easily quantified and correlated to the physical observables studied. Theoretical methods developed for crystalline solids can be readily borrowed and extended to study the disordered systems represented by the QPM.

In a preliminary report,[11] we outlined the construction of the QPM for a-SiO_2 and SiO_x. In this paper we present the new results obtained by the construction and analysis of three inequivalent QPM for a-SiO_2 and for each of the SiO_x with $x=1.5$, 1.0, and 0.5. The models for SiO_x should be of particular interest because they yield the microscopic information about the atomic scale structures and the stoichiometry of the Si-SiO_2 interfacial regions. Currently, there are two competing models for the structures of SiO_x: (1) The microscopic random-bond (RB) model[12] in which the Si—Si and Si—O bonds are statistically randomly distributed throughout the SiO_x structure, and (2) the random-mixture (RM) model[13] in which the tetrahedrally bonded units of a-Si and a-SiO_2 are randomly dispersed and each has a domain size of a few tetrahedral units. We have constructed QPM of SiO_x with $x=1.0$ according to the above two assumptions. Detailed analysis of the two types of models and the subsequent calculation of electronic structures based on these models[14] seems to favor the RB description for SiO_x. Accordingly, the models for SiO_x with $x=0.5$ and $x=1.5$ are constructed according to the RB concept.

In the next section we describe the process of construction of these QPM and comment on some subtleties in the technical details. In Sec. III the results of a-SiO_2 models are presented and compared with the cluster models of Bell and Dean (BD).[1] In Sec. IV A the results of SiO models based on both RB and RM concepts are presented, compared, and contrasted. The results of SiO_x with $x=0.5$ and 1.5 are discussed in Sec. IV B. In the Sec. V we summarize the results and present arguments in favor of the RB model for SiO_x. In the subsequent papers,[14] the detailed electronic structures for a-SiO_2 and SiO_x calculated using these models will be presented.

II. METHOD OF MODEL CONSTRUCTION

In a CRN theory for a covalently bonded glassy material, the atoms maintain short-range order as required by the theory of chemical bonding. The most difficult part in constructing a QPM is to maintain the periodic boundary condition (PBC) across the cell boundary without severely distorting the directional bonding of the atoms involved. No systematic method has yet been developed which gives a unique prescription for constructing such cells with an ensured minimum distortion from the normal bonding structures. Three QPM for tetrahedrally bonded a-Si are in existence; these are either handbuilt or computer assisted and represent the best models out of many trials. The first of such models was built by Henderson and Herman[8] with 61 atoms in the unit cell. A second one with a smaller overall distortion and 54 atoms in the unit cell was constructed by Guttman.[9] Still another model with a somewhat larger distortion was constructed by a group at Yale University;[6] it contained 62 atoms in the unit cell. We shall label these three models as H61, G54, and Y62, respectively.

To construct QPM for a-SiO_2 following an approach similar to that used for a-Si would be even more difficult and time consuming. It is expedient to utilize the existing models for a-Si and to derive a QPM for a-SiO_2 such that the difficulty of matching the PBC can be circumvented. This can be done by inserting O atoms between each pair of Si atoms in the a-Si model and then rescaling the atomic coordinates and the size of the cubic cell such that the density of the a-SiO_2 model corresponds to 2.20 g/cm^3 as measured experimentally. Thus a starting configuration of a QPM of a-SiO_2 is obtained with the network topology and ring structures identical to those of the originating a-Si model. When only a fraction of the available O sites is occupied, we have SiO_x models. If the O sites in a SiO_x model are randomly picked, we have a RB model. If the choice of O sites are biased such that Si—O bonds tend to be locally connected, we have a RM model. These procedures are illustrated with two-dimensional sketches in Fig. 1.

Once the initial configuration for a QPM has been determined, it is necessary to reduce the bond distortion by relaxing the structure under some potential function such that the elastic energy is minimized. It has been argued[15] that a correct potential function for such purpose should yield the structure of quartz for SiO_2 after relaxation since this naturally occurring phase represents one of the most thermodynamically stable structures of SiO_2 and hence possesses the lowest potential energy. However, our purpose is to obtain an acceptable finite CRN structure for a-SiO_2 with the constraints of PBC and with bond length and angle distortion consistent with experimental information. Because we are less concerned about the accuracy of such a potential function or its derivation from first principles, a phenomenological approach is used. We use

a Keating-type potential[16] for both Si and O atoms,

$$V=\sum_l V_l^{\mathrm{Si}}+\sum_n V_n^O , \tag{1}$$

$$V_l^{\mathrm{Si}}=\frac{3}{16}\frac{\alpha}{d^2}\sum_{i=1}^{4}(\vec{r}_{l,i}\cdot\vec{r}_{l,i}-d^2)^2 + \frac{3}{8}\frac{\beta_1}{d^2}\sum_{(i,i')}^{6}(\vec{r}_{l,i}\cdot\vec{r}_{l,i'}-d^2\cos^{-1}\phi)^2 , \tag{2}$$

$$V_n^{\mathrm{O}}=\frac{3}{16}\frac{\alpha}{d^2}\sum_{j=1}^{2}(\vec{r}_{n,j}\cdot\vec{r}_{n,j}-d^2)^2 + \frac{3}{8}\frac{\beta_2}{d^2}\sum_{(j,j')}(\vec{r}_{n,j}\cdot\vec{r}_{n,j'}-d^2\cos^{-1}\theta)^2 , \tag{3}$$

where $\vec{r}_{l,i}$ is the radius vector from atom l to its (NN) atom i, ϕ is the ideal O-Si-O, O-Si-Si, or Si-Si-Si angle (109°27′), θ is the average Si-O-Si angle which is about 147°, and d is the ideal Si—O or Si—Si bond length (1.69 or 2.35 Å) as the case may be. The first term in (2) and (3) is a sum over NN while the second term is a sum over the NN pairs. α is the bond-stretching constant and β_1 and β_2 are the bond-bending constants about the O-Si-O angle and Si-O-Si angle, respectively. The ratio of β_1/α is set equal to 0.17 according to the analysis of Galeener,[17] and β_2 is set to be $\beta_1/3$. In the case of SiO_x models, no distinction is made between bond bendings about O-Si-O, Si-Si-O, or Si-Si-Si angles. In the computer-relaxation process, the force tensor for each atom is calculated from the potential form of Eqs. (1)—(3). Each atom is picked in a random sequence and is moved to a position of zero force. The iteration process stops when the computed deviations of bond length and bond angles have stabilized to one part in 10^5 and a final relaxed QPM structure is obtained. The relaxation process is found to converge rather rapidly since our initial configuration already defines the topology of the network and no bond pattern changes are introduced in the relaxation process. Various test runs

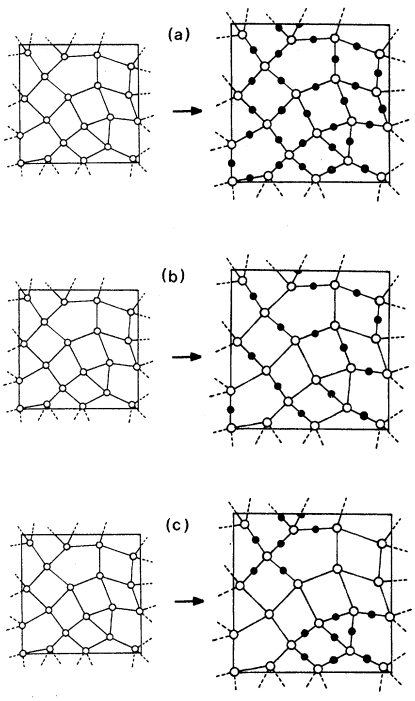

FIG. 1. Schematic illustrations of obtaining initial configurations from the periodic model of a-Si: (a) a-SiO_2, (b) RB model of SiO_x, (c) RM model of SiO_x.

TABLE I. Properties a-SiO_2 models.

Model	G54	H61	Y62	BD	α-quartz	Experiment
No. of atoms	162	183	186	614	9	
Type	periodic	periodic	periodic	cluster	periodic	
Density (g/cm^3)	2.20	2.20	2.20	~1.99	2.65	2.20
$\bar{R}_{\mathrm{O-Si}}$ (Å)	1.62	1.62	1.64	1.620	1.62	1.62
$\Delta R/R$	0.007	0.010	0.017	0.035	0.000	
θ (O-Si-O)	109.3°	109.3°	109.2°	109.30°		
$\Delta\theta$	4.8°	6.8°	8.2°	6.2°		
$\bar{\phi}$ (Si-O-Si)	147.2°	152.3°	151.5°	153.3°	144.0°	144°—152°
$\Delta\phi$	13.8°	14.2°	13.1°	9.6°		
Peak positions in RDF (in Å)						
P_1	1.62	1.62	1.64	1.6		1.61
P_2	2.66	2.68	2.70	2.6		2.64
P_3	3.14	3.17	3.23	3.1		3.06
P_4	4.14	4.16	4.28	4.1		
P_5	5.18	5.63	5.45	5.1		

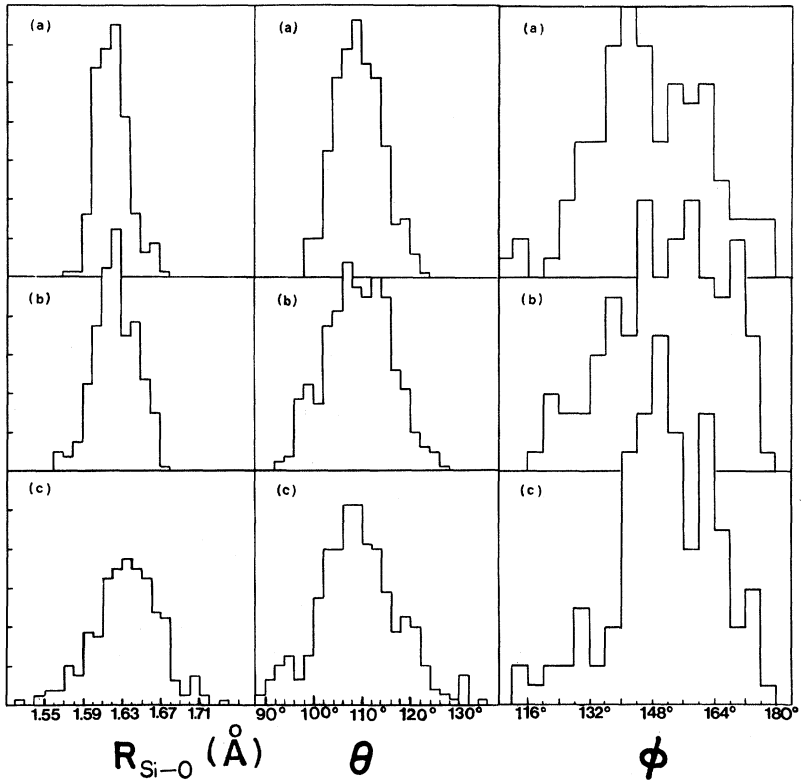

FIG. 2. Distribution of Si—O bond length, tetrahedral angle θ, and bridging angle ϕ for QPM of a-SiO_2: (a) G54, (b) H61, (c) Y62.

indicate that the structure after relaxation is rather insensitive to a reasonable range of choice of the ratios of the parameters α/β_1 and β_1/β_2. Since these models are derived from a-Si models[8–10] which contain no four-member rings, the present QPM for a-SiO_2 also contain no four-member rings. To test the effect of the presence of four-member rings in the structures, several models with various numbers of four-member rings are also constructed by the removal of few Si atoms in the original a-Si model before inserting O atoms and reassigning the affected neighboring atoms. Such models are in general found to have larger distortion after computer relaxation.

III. a-SiO_2 MODELS

For a-SiO_2 models, three QPM were constructed in the manner described in Sec. II, each originating from H61, G54, and Y62 models for a-Si. We shall again label these models as H61, G54, and Y62 for the a-SiO_2; they contain, respectively, 61, 54, and 62 Si atoms and 122, 108, and 124 O atoms. The characteristics of these relaxed models are listed in Table I along with the cluster model of BD,[1] and that of crystalline quartz. This includes density, average bond length, and bond angle, their root-mean-square (rms) deviations of these quantities, and the peak positions in the RDF. To give a better idea about the local short-range order of each model, the distributions of Si—O bonds, O-Si-O tetrahedral angles θ, and Si-O-Si bridging angles ϕ are plotted in Fig. 2. It is apparent that G54 has the smallest overall distortion while Y62 has the largest distortion. This is similar to the original QPM of a-Si and indicates that the distortion in a particular QPM is mainly determined by the topology of the network with the constraint imposed by the PBC. However, the QPM for a-SiO_2 have much smaller distortion than the corresponding a-Si models. For example, in the G54 model, the relative rms value of the NN bond length is 0.03 in a-Si but only 0.007 in a-SiO_2; the rms deviation of the tetrahedral angle θ is 11° in a-Si compared to 4.8° in a-SiO_2. This is attributed to the flexibility of the Si-O-Si bridging angles in the a-SiO_2 network. In comparing our QPM with the mechanically con-

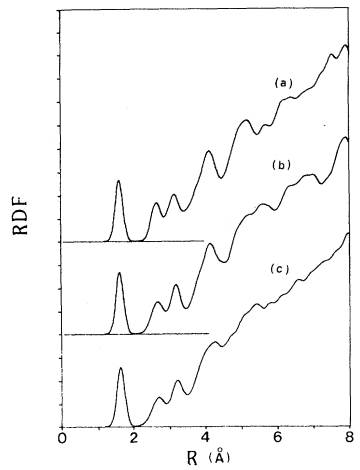

FIG. 3. X-ray RDF computed from the QPM of a-SiO_2: (a) G54, (b) H61, (c) Y62. For each pair counted, Gaussian broadening of halfwidth of 0.1 Å is applied. This is true for all subsequent RDF and partial RDF calculations.

structed model of BD which has a much lower density than the experimental value, we notice that BD has a much larger bond-length distortion, a smaller bridging angle distortion, and an intermediate distortion for the tetrahedral angles θ. The average bridging angles $\bar{\phi}$ obtained from the three models

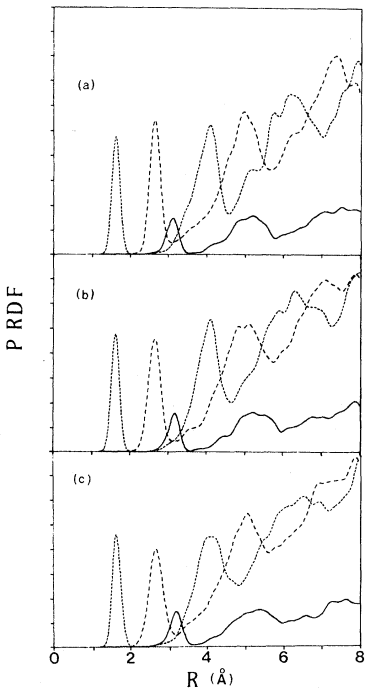

FIG. 4. Partial pair distribution function for a-SiO_2. Solid line, Si-Si pairs; dotted line, O-Si pairs; dashed line O-O pairs. (a) G54, (b) H61, (c) Y62.

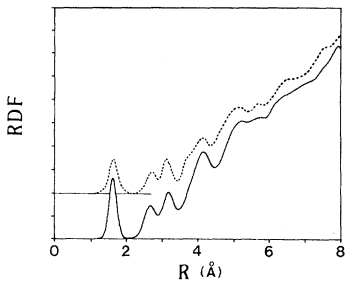

FIG. 5. Solid line, averaged x-ray RDF of the three QPM. Dashed line, experimental RDF from Ref. 1.

(147.2°,152.3°,151.5°) are slightly smaller than the BD model (153.3°). The most contrasting property of BD model is that it contains 19% of four-member rings. Our QPM, being derived from a-Si models, contain no four-member rings. Other cluster models[4] of a-SiO_2 contain less than 1% of four-member rings. BD had pointed out that the presence of four-membered rings is important to account for a shoulder in the RDF at 3.8 Å. We have analyzed our QPM with some four-member rings by the method of removing some Si atoms in the a-Si model and reassigning bonds before relaxing. The RDF thus calculated did show a slight shoulder at 3.7 Å, but it was not as prominent as in the BD model. In view of the large density deficit of the BD model and the fact that recent electron diffraction data show less sign of the shoulder,[18] and a more careful analysis of the experiment RDF,[19] we conclude that the presence of four-member rings in a-SiO_2 is unquestionable, but probably less than a few percent.

The RDF of a-SiO_2 had been measured by many people[18–23] using x-ray, neutron, and electron diffraction methods. In Fig. 3 we plot the x-ray RDF calculated for the three QPM from 0–8 Å. Atomic scattering factors of 14.75 and 7.625 electrons are used for Si and O atoms, respectively, as was done in Ref. 1. Because of the quasiperiodicity of the models, we are able to calculate the RDF up to any range without additional correction for the surface effect as would be needed in a finite-cluster model. In order to have a better insight on the various structures in the RDF, we resolve the pair distributions in the O-O, O-Si, and Si-Si components for each of the three QPM. These are shown in Fig. 4. By taking G54 as an example, the first three peaks in the RDF at 1.62, 2.66, and 3.14 Å are from Si-O, O-O, and Si-Si pairs, respectively; beyond 4.0 Å, all pairs contribute to the structure with Si-O and O-O pairs mainly responsible for peaks at 4.14 and 5.18 Å, respectively. The other two models gave similar

results with Y62 having peaks at higher positions. In Fig. 5, we compare the average x-ray RDF of the three QPM with the averaged experimental RDF.[1] The agreement can be regarded as excellent. Not only the positions of the major peaks are matched, but also the smaller structures beyond 5. Angstroms are quite well reproduced. The same good agreement in RDF has also been obtained by the BD model although the BD model has some characteristics quite different from the QPM. This indicates that the RDF is an averaged physical quantity which may not serve as a test stringent enough to distinguish the subtleties in the different structural models.

IV. AMORPHOUS SiO_x MODEL

The structure of SiO_x films and Si-SiO_2 interfaces has been receiving much attention in recent years.[18,24–35] Several possible structural models have been suggested based on the analysis of the results obtained from various experimental investigations.[12,13,18] It is possible that any one of them may be valid under a particular preparation condition. We are mainly concerned here with the atomic level structure of powder-deposited SiO_x films and the question of whether the same SiO_x structure is appropriate for the interface of Si and SiO_2. Auger spectroscopy[24] indicates that a layer of SiO_x of width about 25–35 Å exists at such an interface with x varying from 0.0 to 2.0 in going from the Si side to the SiO_2 side. The main controversy is at what level Si and SiO_2 are mixed. The random-mixture model[13] suggests the mixing of SiO_2 and Si at the level of several tetrahedral units while the microscopic random-bond model[12] assumes a complete mixing of Si–Si and Si–O bonds with fourfold tetrahedral bonding for Si atoms and a twofold bridging bond for O atoms as the only constraint. Temkin,[13] based on the analysis of x-ray diffraction data of Yasaitis and Kaplow (YK)[25] concluded that the RM model is the appropriate one. Nevertheless, the most conclusive evidence can be obtained only when we actually construct physical models according to the above two competing concepts, analyze the resulting model structures, and then compare with diffraction data and all other available information.

A. SiO_x models, $x=1$

We constructed SiO_x models as described in Sec. II for both RM and RB models. The size of the supercell with $a=12.23$ Å is determined by the density of SiO which was measured to be 2.15 g/cm^3.[25,26] Three similar but inequivalent models are constructed for each case by changing random-initial configurations. Each Si atom in SiO_x can bond to n O atoms and $(4-n)$ Si atoms where $n=0,1,2,3,4$. Following Temkin, we denote the fraction of each of the five tetrahedral units to be C_i with i ranging from 1 to 5. These parameters C_i are of considerable importance since they determine the manner in which the Si and O atoms are admixed. These and other properties for SiO_x with $x=1$ are listed in Table II for both RM and RB models.

To compare the two types of the SiO_x models, we have plotted the distribution of Si-O bond, Si–Si bond, tetrahedral angle θ, and the Si-O-Si bridging angle ϕ in Fig. 6. In general, the distortions of angles θ and Si–O bonds are about the same in these two models. The RM model has a larger Si–Si bond distortion as well as a larger spread of angle ϕ distribution. Furthermore, the mean Si–O bond distance is shorter in the RM model than in the RB model. In Fig. 7 we plot the x-ray RDF for each type of model together with the relevant x-ray diffraction data[25] for $x=1.06$. There appears to be no drastic difference in the RDF for the two models. The only difference seems to be that the RB model has a slightly more prominent third peak at 3.38 Å

TABLE II. Properties of SiO_x, $x=1$ model.

	RB (3 each)	RM (3 each)
No. of Si atoms	54	54
No. of O atoms	54	54
Density (g/cm^3)	2.15	2.15
$\bar{R}_{O-Si}$ (Å)	1.67	1.64
$\frac{\Delta R}{R}$ for O-Si	0.045	0.027
$\bar{R}_{Si-Si}$ (Å)	2.45	2.52
$\frac{\Delta R}{R}$ for Si-Si	0.052	0.089
$\bar{\theta}$ (X-Si-X, X=O or Si)	108.6°	108.7°
$\Delta\theta$	13.3°	13.5°
$\bar{\phi}$ (Si-O-Si)	157.0°	152.2°
$\Delta\phi$	16.4°	16.0°
C_1	0.080	0.191
C_2	0.241	0.290
C_3	0.358	0.169
C_4	0.241	0.031
C_5	0.080	0.321
P_1 (Å)	1.65	1.63
P_2 (Å)	2.46	2.52
P_3 (Å)	3.38	3.43
P_4 (Å)	4.3–4.75	4.76

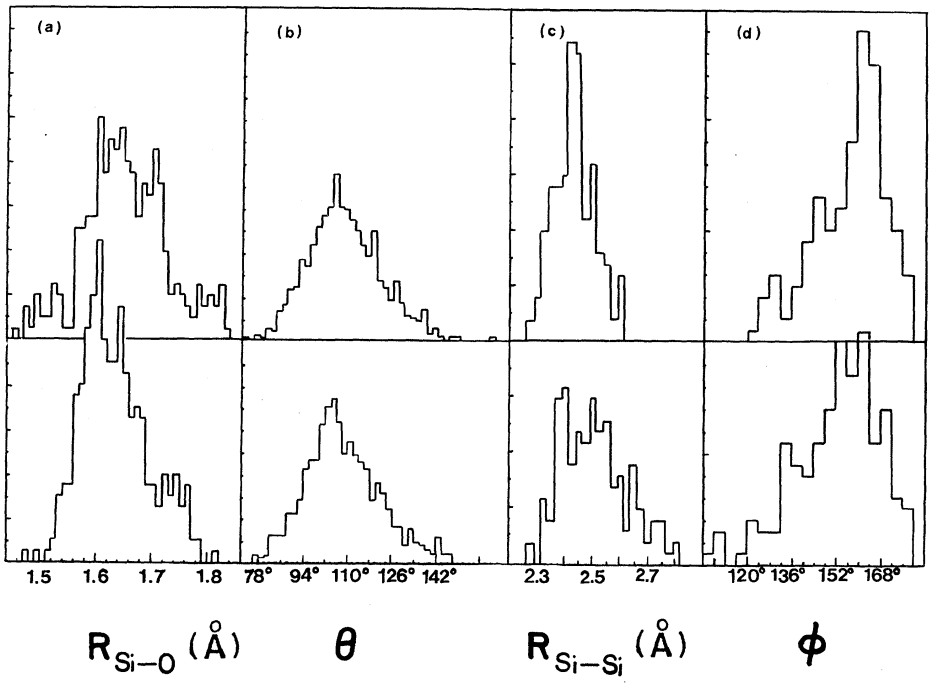

FIG. 6. Distribution of (a) Si—O bond, (b) tetrahedral angle θ, (c) Si—Si bond, (d) bridging angle ϕ for SiO_x, $x=1$ models. Upper panels, RB model; lower panels, RM model.

and broader fourth peak between 4.3—4.8 Å. The fourth peak, which was quite prominent in the experimental data, was less evident in the RB model. Furthermore, in the RB model the Si-Si peak at 2.46 Å is stronger than the Si-O peak at 1.65 Å, as was found experimentally, while in the RM model, these two peaks (at 2.52 and 1.63 Å) are about the same height. Based on these facts, it appears that the RB model should be slightly favored over the RM model although the differences in the two RDF are quite small. We shall return to discuss this point in the next section. In Fig. 8 we resolve the RDF of both models into their partial components. This reveals the fact that the second peak arises from both Si-Si and O-O pairs. For structures beyond the second peak, all pairs contribute and the structure in the RDF cannot be analyzed in a sim-

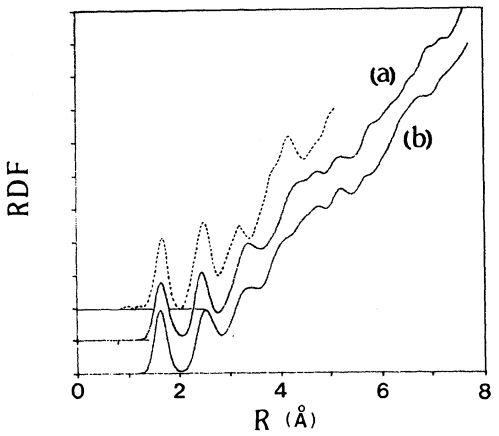

FIG. 7. X-ray RDF calculated for SiO_x, $x=1$: (a) RB model, (b) RM model. Dashed line, experimental data of Ref. 24.

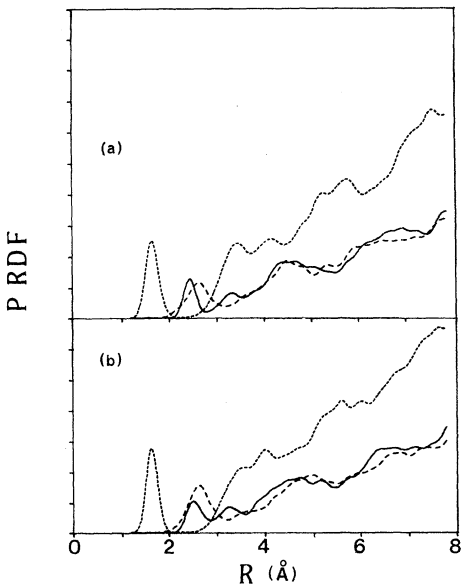

FIG. 8. Partial pair distribution functions for SiO_x. $x=1$, (a) RB model, (b) RM model. Notations are the same as Fig. 4.

TABLE III. Properties of SiO_x models, $x=0-2.0$.

x	$x=2.0$	$x=1.5$	$x=1.0$	$x=0.5$	$x=0$
No. of Si atoms	54	54	54	54	54
No. of O atoms	108	87	54	27	0
Density (g/cm^3)	2.20	2.15	2.16	2.28	2.40
$\bar{R}_{O-Si}$ (Å)	1.62	1.65	1.67	1.64	
$\Delta R_{O-Si}/R_{O-Si}$	0.007	0.025	0.045	0.039	
$\bar{R}_{Si-Si}$		2.42	2.45	2.42	2.35
$\Delta R_{Si-Si}/R_{Si-Si}$		0.034	0.052	0.040	0.025
$\bar{\theta}$ (tetrahedral)	109.3°	109.1°	108.6°	108.5°	109.4°
$\Delta\theta$	4.8°	10.5°	13.3°	13.3°	13.0°
$\bar{\phi}$ (Si-O-Si)	147.2°	154.3°	157.0°	153.9°	
$\Delta\phi$	13.8°	14.5°	16.4°	16.9°	
C_1	0.0	0.0	0.080	0.395	1.0
C_2	0.0	0.068	0.241	0.333	0.0
C_3	0.0	0.173	0.358	0.241	0.0
C_4	0.0	0.451	0.241	0.037	0.0
C_5	1.0	0.309	0.080	0.019	0.0

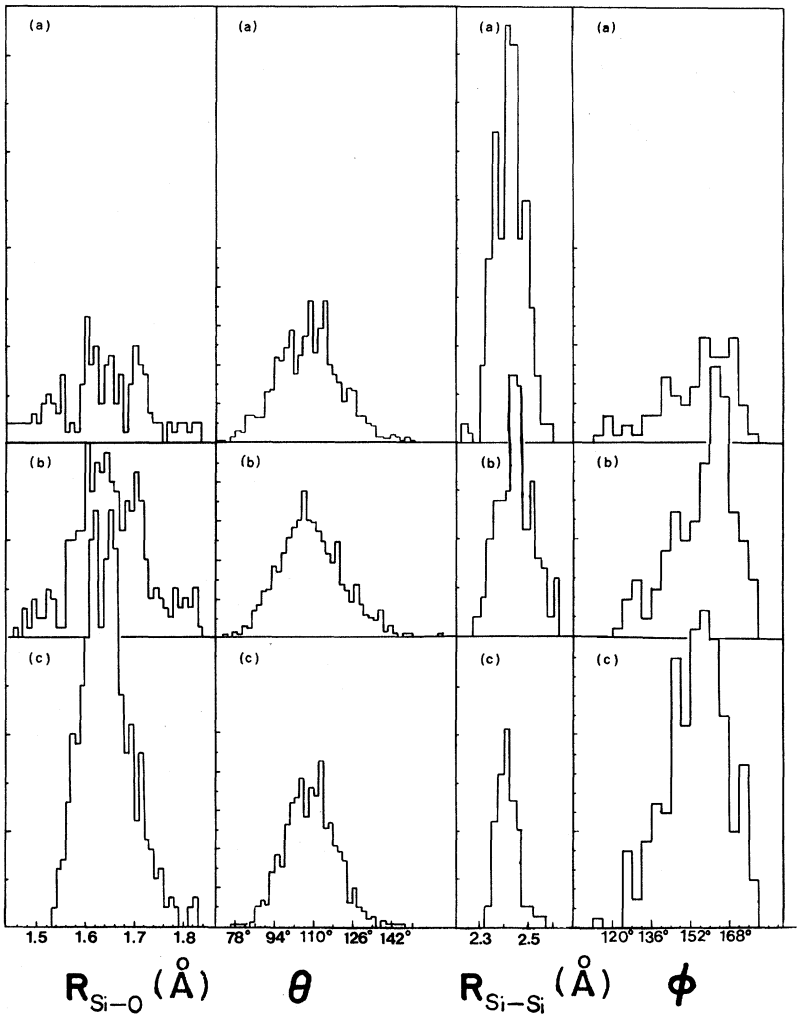

FIG. 9. Bond-length and bond-angle distribution for RB model of SiO_x: (a) $x=1.5$, (b) $x=1.0$, (c) $x=0.5$. Notations are the same as Fig. 6.

ple manner based only on a few standard bonding configurations.

B. SiO_x models, $x = 0.5$ and 1.5

From models of SiO_x with $x = 1.0$, it was shown that the RDF's for both the RB model and the RM model are not significantly different, with the RDF from the former in slightly closer agreement with experimental data. Accordingly, we constructed three inequivalent models each for $x = 0.5$ and $x = 1.5$ based on the concept of the RB model. The size of the quasiperiodic cells are chosen to be 11.24 and 12.95 Å, respectively, so that the density of SiO_x for $x = 0.5$ and $x = 1.5$ will be 2.28 and 2.15 g/cm^3. These are the interpolated values between the densities of a-Si (2.33 g/cm^3), SiO (2.16 g/cm^3), and a-SiO_2 (2.20 g/cm^3). The parameters of these models, together with that of $x = 1.0$ and the G54 model of a-SiO_2 and a-Si, are listed in Table III for comparison. It is to be noted that in general for SiO_x the average Si—O bond length is larger than the ideal Si—O bond length of 1.62 Å as in a-SiO_2, while the Si—Si bond length is larger than the ideal length of 2.35 Å as in a-Si. This elongation of bonds is largest in the case of $x = 1$. Thus the effect of additional disorder introduced in SiO_x is to elongate the normal Si—O and Si—Si bond lengths.

The distributions of bond length and bond angles for $x = 1.5$, 1.0, and 0.5 models are shown in Fig. 9. The scales in this figure are such that the area under the curve represents the actual number of bonds or angles in each type of the model. As x increase from 0.5 to 1.5, the distortions of angles remain relatively the same. In comparing these distributions with those of a G54 model of a-SiO_2 in Fig. 2 and that of a-Si of Ref. 8, we realize that the bond and angle distortions are much smaller in the cases of a-SiO_2 and a-Si. Thus the chemical composition of a-SiO_x where x is neither 0 nor 2, introduces additional disorder which results in a larger distortion of bond lengths and bond angles. This effect is more evident on the low-x side than on the high-x side.

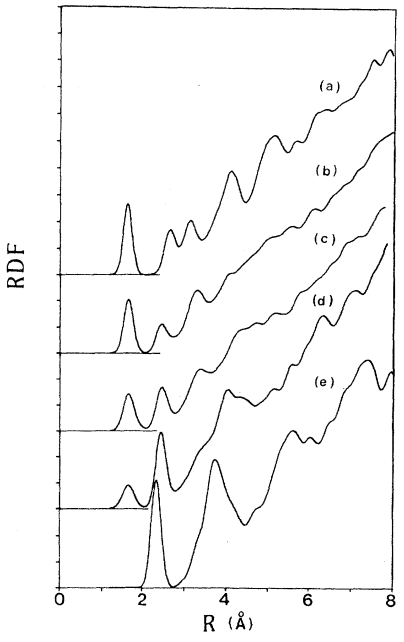

FIG. 10. X-ray RDF for SiO_x: (a) $x = 2.0$ (a-SiO_2), (b) $x = 1.5$, (c) $x = 1.0$, (d) $x = 0.5$, (e) $x = 0$ (a-Si).

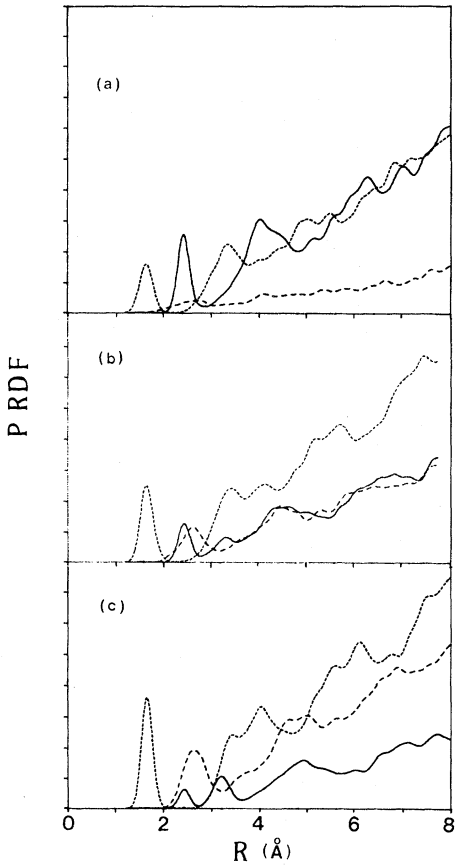

FIG. 11. Partial pair distribution functions for SiO_x: (a) $x = 1.5$, (b) $x = 1.0$, (c) $x = 0.5$. Notations are the same as Fig. 4.

In Fig. 10 we display the RDF for SiO_x for $x = 2.0$ to $x = 0$. From these curves it is apparent that the Si-O peak diminishes and the Si-Si peak grows and shifts from 2.67 to 2.32 Å in going from a-SiO_2 to a-Si. Structures below 4 Å are present in all curves as a result of the basic chemical bonding of NN atoms and are similar for all the models. Beyond the 4-Å range, only a-SiO_2 and a-Si have

well-defined peak structures. For $x=1.5$ and 1.0 the RDF is rather featureless beyond 4 Å. In Fig. 11 the partial RDF for $x=0.5$, 1.0, and 1.5 are displayed in order to better display the nature of various structures in the RDF.

V. DISCUSSION

Although construction of structural models for a-SiO_2 started more than 15 years ago, the present results are the first time that finite models with PBC have been constructed for a-SiO_2. The RDF computed from these models agrees well with experimental x-ray diffraction data. With the QPM, the density of the model can always be adjusted to the correct measured value and the physical characteristics of each model analyzed in detail. With three inequivalent models with different degrees of distortions, we shall be able to study other properties of a-SiO_2 based on these models and correlate them with their different structural characteristics. The periodicity of the model enables us to deal with the complicated disordered system with theoretical methods developed for crystalline solids. This line of approach seems to be very fruitful in theoretical studies of disordered systems and has already been demonstrated to be quite successful in the case of amorphous semiconductors[10,36] and glasses.[37]

For SiO_x models we start with $x=1$. Both the RM models and RB models have been constructed and their statistical bond pattern analyzed. The RDF of these two types of model are shown to be quite similar with RB in closer agreement with experiment. Temkin[11] had concluded from the data of YK (Ref. 25) that the RM model is the more appropriate one for SiO. However, in looking deeper into Temkin's theory, we observed several deficiencies:

(1) In the six types of NN and next-NN bond patterns considered by Temkin, the O-Si-O and Si-O-Si angles are assumed to have their ideal values of 109.5° and 144°, respectively, while in reality, a distribution of angles such as those shown in Fig. 6 needs to be considered.

(2) The value of the parameter C_i for $i=1$ to 5 can be rather easily obtained for an RB model based solely on statistical arguments, but it is far more difficult to obtain C_i for an RM model from purely theoretical deduction. In RM models each Si-like and SiO_2-like region is at most a few tetrahedral units in extent. There is a substantial boundary region to be considered in determining the parameters C_i. In Fig. 12 we plot the C_i values for $x=0.5$, 1.0, and 1.5 for RB models, as well as for $x=1.0$ for RM models. The values for C_i obtained from the present modest-size RB models are in good agreement with the exact statistical prediction,[11] while for the RM model with $x=1.0$, the C_i values ($C_1=0.191$, $C_2=0.290$, $C_3=0.167$, $C_4=0.031$, $C_5=0.321$) are significantly different from those assumed by Temkin ($C_1=C_5=\frac{1}{3}$, $C_2+C_3+C_4=\frac{1}{3}$) in his analysis.

(3) Temkin's strongest argument against the random model in favor of the mixture model came from the calculated area of the third peak in the RDF. However, by neglecting all bond patterns beyond the second NN and the use of imprecise C_i values, the area for the third peak in RDF determined by the Temkin model is incorrect. The partial RDF of Fig. 8 clearly indicates the substantial contribution for higher-order bond patterns. The approximate areas of the third peak in both models are actually quite close as shown in Fig. 7. Recent electron diffraction study of SiO_x films for $x=1.06$ by George and D'Antonio[18] (GD) indicated the position of the Si-Si peak and the O-O peak to be at 2.36 and 2.63 Å, respectively. The corresponding values from Fig. 8 are 2.44 and 2.63 Å for the RB model and 2.49 and 2.63 Å for the RM model. This gives more evidence that RB is in better agreement with experiment than the RM. However, GD used the same analysis as Temkin's to draw an opposite conclusion. Very recently, Engelke *et al.*[38] performed a high-intensity x-ray diffraction measurement. From an extensive analysis of the RDF obtained, they found that the RB model will fit the experimental data best, especially when some defect

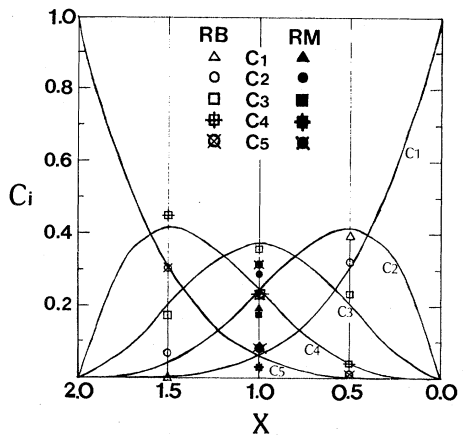

FIG. 12. Probability of the ith tetrahedral configuration, C_i. Solid lines, exact theoretical result for RB model. Open symbols values of C_i obtained from the RB QPM. Solid symbols, C_i values from RM model with $x=1$.

centers simulated by O—O bonds are included. Philipp reported[12] that in his optical experiments, a continuous range of Si to O deposition ratio is possible for SiO_x films that exhibit a continuous range of absorption coefficients. He suggested that this is more consistent with the RB model line of thinking than the RM model. Furthermore, the distribution diagram in Fig. 6 indicates that in general, RM models have larger bond-length and bond-angle distortions, and hence, possess greater strain energy in the network than the RB models. No well-characterized structural measurements for SiO_x with x close to 0.5 or 1.5 exist. Although GD reported electron diffraction data for SiO_x with $x=0.84$ and 1.27 in addition to $x=1.06$, it is highly desirable that similar structural determination be done for $x=0.5$ and $x=1.5$ to check out the reliability of the models constructed.

The models presented in this paper are constructed on the notion of CRN, which is the lowest level of description for the highly complicated structure of glasses and precludes other recently suggested but more sophisticated structural models involving clusters,[39] internal microvoids,[2] reconstruction,[40] and particular forms of dislocations or defect centers. The approach of systematic construction and analysis of QPM can, however, be readily extended to make quantitative tests of those newly suggested theories. This approach can also be employed for the study of more complicated systems such as those involving alkali-metal ions in silicate glasses. In conjunction with first-principles quantum-mechanical calculations of electron states on the suitably constructed QPM, a closer comparison with other experimental measurements would become possible and deeper insight about the nature of disordered systems can be obtained. This will serve as a much more stringent test for the model structure than simply demanding a good agreement on RDF which is only an averaged quantity.

As mentioned earlier, the most difficult part in constructing QPM is to match the bonds at the supercell boundary and to my knowledge, no efficient systematic scheme has been developed which can produce the periodic model for covalently bonded noncrystalline materials without consuming a prohibitive amount of either human labor or computer time. Should such a scheme be available, theoretical study of many different disordered systems via the construction of a suitable QPM can be much more fruitful. The situation may be more promising in amorphous metals or metallic alloys. Unlike covalently bonded oxide glasses or amorphous semiconductors which require a stringent local directional bonding to match at the boundary, the boundary for a metal or alloy depends only on the NN species and the coordination number; this makes the PBC condition easier to maintain. Also, a simple pairwise interatomic potential, such as the Lennard-Jones type will be applicable in the computer relaxation process. Work on metallic glasses using such an approach has already been started.[41] Previously, the structure of metallic glasses has always been described by large finite-cluster models.[42,43] Systematic study of this important class of materials as well as other covalently bonded disordered systems using a QPM approach will be an important task for future years.

ACKNOWLEDGMENT

This work is supported by a Department of Energy Contract No. DE-AC02-79ER10462.

[1]R. J. Bell and P. Dean, Philos. Mag. 25, 1381 (1972).
[2]J. C. Phillips, Phys. Status Solidi B 101, 473 (1980); Phys. Rev. B 24, 1744, (1981).
[3]Y. Bando and K. Ishizuka, J. Non-Cryst. Solids 33, 375 (1979).
[4]F. Ordway, Science 143, 800 (1964); D. L. Evans and S. V. King, Nature (London) 212, 1353 (1966); R. J. Bell and P. Dean, *ibid.* 212, 1354 (1966).
[5]D. E. Polk, J. Non-Cryst. Solids, 5, 365 (1971); D. E. Polk and D. S. Boudreaux, Phys. Rev. Lett. 31, 92 (1973); G. A. N. Connell and R. J. Temkin, Phys. Rev. 9, 5223 (1974).
[6]P. Steinhardt, R. Alben, and D. Weaire, J. Non-Cryst. Solids 15, 199 (1974).
[7]G. N. Greaves and E. A. Davis, Philos. Mag. 29, 1201 (1974); S. R. Elliott and E. A. Davis, in *Structure and Excitations of Amorphous Solids—1976 (Williamsburg, Virginia)*, Proceedings of an International Conference on Structure and Excitation of Amorphous Solids, edited by G. Lucovsky and F. L. Galeener (AIP, New York, 1976), pp. 117, A. L. Renninger, M. D. Rechtin, and B. L. Averbach, J. Non-Cryst. Solids 16, 1 (1974).
[8]D. Henderson, J. Non-Cryst. Solids, 16, 317 (1974); D. Henderson and F. Herman, *ibid.* 8-10, 359 (1972).
[9]L. Guttman, Bull. Am. Phys. Soc. 22, 64 (1977).
[10]W. Y. Ching, C. C. Lin, and L. Guttman, Phys. Rev. B

16, 5488 (1977).
[11]W. Y. Ching, in *Physics of* MOS *Insulators,* edited by G. Lucovsky, S. T. Pantelides, and F. L. Galeener (Pergamon, New York, 1980), p. 63.
[12]H. R. Philipp, J. Non-Cryst. Solids, 8-10, 627 (1972); J. Phys. Chem. Solids 32, 1935 (1971).
[13]R. J. Temkin, J. Non-Cryst. Solids, 17, 215 (1975).
[14]W. Y. Ching, following paper, Phys. Rev. B 26, 6622 (1982); this issue, 26, 6610 (1982).
[15]F. Herman (private communication).
[16]P. N. Keating, Phys. Rev. 145, 637 (1966).
[17]F. L. Galeener, Phys. Rev. B 19, 4292 (1979).
[18]C. F. George and P. D'Antonio, J. Non-Cryst. Solids 34, 323 (1979).
[19]J. R. G. DaSilva, D. G. Pinatti, C. E. Anderson, and M. L. Radee, Philos. Mag. 31, 713 (1975).
[20]E. H. Henninger, R. C. Buschart, and L. Heaton, J. Phys. Chem. Solids 28, 423 (1967).
[21]R. L. Mozzi and B. E. Warren, J. Appl. Crystallogr. 2, 164 (1969).
[22]J. H. Konnert and J. Karle, Acta Crystallogr. Sect. A 29, 702 (1973).
[23]M. V. Coleman and D. J. D. Thomas, Phys. Status Solidi 22, 593 (1967).
[24]J. S. Johamessen, W. E. Spicer, and Y. E. Strausser, Thin Solid Films 32, 311 (1976).
[25]J. A. Yasaitis and R. Kaplow, J. Appl. Phys. 43, 995 (1972).
[26]S. C. H. Lin and M. Joshi, J. Electrochem. Soc. Solid State Sci. 116, 1740 (1969).
[27]M. T. Costa Lima and C. Senemand, Chem. Phys. Lett. 40, 157 (1976).
[28]T. H. DiStefano, J. Vac. Sci. Technol. 13, 856 (1976).
[29]G. Hollinger, Y. Jugnet, and Tran Minh Duo, Solid State Commun. 22, 277 (1977).
[30]G. Hollinger, thèse de Doctoral d'Etat, Université Claude Bernard, Lyon, 1979 (unpublished).
[31]F. J. Grunthaner, P. J. Grunthaner, R. P. Vasquez, B. F. Lewis, J. Maserjian, and A. Madhukar, Phys. Rev. Lett. 43, 1683 (1979); J. Vac. Sci. Technol. 16, 1443 (1979).
[32]T. Adachi and C. R. Helms, Appl. Phys. Lett. 35, 199 (1979).
[33]A. Ishizaka and S. Iwata, Appl. Phys. Lett. 36, 71 (1980).
[34]I. Ito, M. Iwani, and A. Hiraki, Solid State Commun. 36, 695 (1980).
[35]R. Carius, R. Fischer, E. Holzenkämpfer, and J. Stuke, J. Appl. Phys. 52, 4242 (1981).
[36]W. Y. Ching and C. C. Lin, Phys. Rev. Lett. 34, 1223 (1975); Phys. Rev. B 18, 6829 (1978).
[37]W. Y. Ching, Phys. Rev. Lett. 46, 607 (1981).
[38]R. Engelke, Th. Roy, H.-G. Neumann, and K. Hübner, Phys. Status Solidi A 65, 271 (1981).
[39]M. H. Cohen and G. S. Grest, Phys. Rev. Lett. 45, 1271 (1980).
[40]C. T. White and K. L. Ngai, Surf. Sci. 98, 227 (1980).
[41]S. S. Jaswal and W. Y. Ching, Bull. Amer. Phys. Soc. 26, 248 (1981); S. S. Jaswal, W. Y. Ching, D. J. Sellmyer, and P. Edwardson, Solid State Commun. 42, 247 (1982).
[42]W. Y. Ching and C. C. Lin, in *Amorphous Magnetism II,* edited by R. A. Levy and R. Hasegawa (Plenum, New York, 1977), p. 469.
[43]D. S. Boudreax, Phys. Rev. B 23, 1506 (1981), and references cited therein.